



This discussion paper is/has been under review for the journal Atmospheric Chemistry and Physics (ACP). Please refer to the corresponding final paper in ACP if available.

A WRF simulation of the impact of 3-D radiative transfer

K. N. Liou et al.

A WRF simulation of the impact of 3-D radiative transfer on surface hydrology over the Rocky–Sierra Mountains

K. N. Liou¹, Y. Gu¹, L. R. Leung², W. L. Lee³, and R. G. Fovell¹

¹Joint Institute for Regional Earth System Science and Engineering, Department of Atmospheric and Oceanic Sciences, University of California, Los Angeles, CA 90095, USA

²Pacific Northwest National Laboratory, Richland, WA, USA

³Research Center for Environmental Changes, Academia Sinica, Taipei, Taiwan

Received: 3 July 2013 – Accepted: 14 July 2013 – Published: 23 July 2013

Correspondence to: Y. Gu (gu@atmos.ucla.edu)

Published by Copernicus Publications on behalf of the European Geosciences Union.

Title Page

Abstract

Introduction

Conclusions

References

Tables

Figures



Back

Close

Full Screen / Esc

Printer-friendly Version

Interactive Discussion



Abstract

Essentially all modern climate models utilize a plane-parallel (PP) radiative transfer approach in physics parameterizations; however, the potential errors that arise from neglecting three-dimensional (3-D) interactions between radiation and mountains/snow on climate simulations have not been studied and quantified. This paper is a continuation of our efforts to investigate 3-D mountains/snow effects on solar flux distributions and their impact on surface hydrology over the Western United States, specifically the Rocky and Sierra-Nevada Mountains. We use the Weather Research and Forecasting (WRF) model applied at a 30 km grid resolution with incorporation of a 3-D radiative transfer parameterization covering a time period from 1 November 2007 to 31 May 2008 during which abundant snowfall occurred.

Comparison of the 3-D WRF simulation with the observed snow water equivalent (SWE) and precipitation from Snowpack Telemetry (SNOTEL) sites shows reasonable agreement in terms of spatial patterns and daily and seasonal variability, although the simulation generally has a positive precipitation bias. We show that 3-D mountain features have a profound impact on the diurnal and monthly variation of surface radiative and heat fluxes and on the consequent elevation-dependence of snowmelt and precipitation distributions. In particular, during the winter months, large deviations (3-D–PP) of the monthly mean surface solar flux are found in the morning and afternoon hours due to shading effects for elevations below 2.5 km. During spring, positive deviations shift to earlier morning. Over the mountain tops above 3 km, positive deviations are found throughout the day, with the largest values of 40–60 W m⁻² occurring at noon during the snowmelt season of April to May. The monthly SWE deviations averaged over the entire domain show an increase in lower elevations due to reduced snowmelt, leading to a reduction in cumulative runoff. Over higher elevation areas, positive SWE deviations are found because of increased solar radiation available at the surface. Overall, this study shows that deviations of SWE due to 3-D radiation effects range from an increase of 18 % at the lowest elevation range (1.5–2 km) to a decrease of 8 % at the

ACPD

13, 19389–19419, 2013

A WRF simulation of the impact of 3-D radiative transfer

K. N. Liou et al.

Title Page

Abstract

Introduction

Conclusions

References

Tables

Figures

◀

▶

◀

▶

Back

Close

Full Screen / Esc

Printer-friendly Version

Interactive Discussion



A WRF simulation of the impact of 3-D radiative transfer

K. N. Liou et al.

Title Page

Abstract

Introduction

Conclusions

References

Tables

Figures

◀

▶

◀

▶

Back

Close

Full Screen / Esc

Printer-friendly Version

Interactive Discussion



highest elevation range (above 3 km). Since lower elevation areas occupy larger fractions of the land surface, the net effect of 3-D radiative transfer is to extend snowmelt and snowmelt-driven runoff into the warm season. Additionally, because about 60–90 % of water resources originate from mountains worldwide, the aforementioned differences in simulated hydrology due solely to 3-D interactions between solar radiation and mountains/snow merit further investigation in order to understand the implications to modeling mountain water resources and their vulnerability to climate change and air pollution.

1 Introduction

The spatial orientation and inhomogeneous features of mountains/snow interact with direct and diffuse solar beams in an intricate manner. Quantifying these interactions and reliably determining total surface solar fluxes for incorporation in a land surface model has been a challenging task that has yet to be accomplished in regional and global climate modeling. Virtually all current climate models have used a plane-parallel (PP) radiative transfer program to perform radiation parameterization, and the potential errors have never been quantified.

In conjunction with radiative transfer in mountains/snow regions, we have developed a Monte Carlo photon tracing program, which is specifically applicable to intense and complex inhomogeneous mountains. We demonstrate that the effect of mountains on surface radiative balance is substantial in terms of subgrid variability as well as domain average conditions – a significant solar flux deviation of $\sim 10\text{--}35\text{ W m}^{-2}$ from the plane-parallel radiation parameterization of conventional climate models would occur if realistic mountain features were accounted for in surface energy modeling (Liou et al., 2007; Lee et al., 2011, 2012). Because of the computational burden required by the 3-D Monte Carlo photon tracing program, an innovative parameterization approach in terms of deviations from the PP radiative transfer results, which are readily available in climate models, was developed for the five components of surface solar flux: direct

A WRF simulation of the impact of 3-D radiative transfer

K. N. Liou et al.

Title Page

Abstract

Introduction

Conclusions

References

Tables

Figures

◀

▶

◀

▶

Back

Close

Full Screen / Esc

Printer-friendly Version

Interactive Discussion

and diffuse fluxes, direct- and diffuse-reflected fluxes, and coupled flux, which involves mountain interactions (Lee et al., 2011). In the development of 3-D radiation parameterization in terms of deviations from PP results, we adopted the mean values for the sky view factor, the terrain configuration factor, the cosine of the solar zenith angle, and conventional topographic parameters for a pre-selected 10 km × 10 km domain involving mean elevation and slope in multiple linear regression analysis, along with their standard deviation and skewness. We used a rugged area of the Sierra Nevada Mountains as an experimental testbed for this development (Lee et al., 2011). Five regression equations for flux deviations, which are linear and have a general 5 by 5 matrix form, have been derived. The flux components computed from Monte Carlo simulations were used to assess the accuracies of multiple regression analysis results for the five flux components, along with multiple determination coefficients R^2 , with a number of surface albedos. The most significant term is the direct flux, which generally has high correlations of > 0.9 with root mean square errors less than 3 W m^{-2} (out of 700 W m^{-2}). Deviations from plane-parallel results are on the order of 100 W m^{-2} . For other flux components, R^2 ranges between 0.6–0.9 and deviations are on the order of a few W m^{-2} .

The preceding 3-D radiative transfer parameterization was incorporated into the WRF model (Skamarock et al., 2005) to investigate and understand the impact of the spatial and temporal distribution and variation of surface solar fluxes on land-surface processes (Gu et al., 2012). The model domain selected for the study was the Sierra Nevada Mountain range, which is centered at 35° N – 120° W and covers the area from 135 – 105° W and 20 – 45° N . 48 h model integrations have been performed starting on 29 March 2007, at 00:00 UTC. We showed that the mountain effect could produce up to -50 to $+50 \text{ W m}^{-2}$ deviations in downward surface solar fluxes over mountain areas, resulting in a temperature increase of up to 1° C on the sunny side. Surface sensible and latent heat fluxes are modulated accordingly to compensate for the change in surface solar fluxes. SWE and surface albedo both show decreases on the sunny side of the mountains, indicating more snowmelt and hence reduced snow albedo associated

**A WRF simulation of
the impact of 3-D
radiative transfer**

K. N. Liou et al.

Title Page

Abstract

Introduction

Conclusions

References

Tables

Figures

◀

▶

◀

▶

Back

Close

Full Screen / Esc

Printer-friendly Version

Interactive Discussion

with more solar insolation due to the mountain effect. The day-averaged deviations in the surface solar flux are positive over the mountain areas and negative in the valleys, with a range between -12 to $+12 \text{ W m}^{-2}$. Differences in the domain-averaged diurnal variation over the Sierras illustrate that mountain areas receive more solar flux during early morning and late afternoon, resulting in enhanced sensible heat and latent heat fluxes from the surface and a corresponding increase in surface skin temperature.

In this paper, we investigate the longer term effect of 3-D radiative transfer over mountains/snow in the Western United States covering both the narrow coastal Sierra-Nevada Range and the broad continental Rocky Mountains. Marked by complex terrain and with surface hydrology dominated by seasonal precipitation and snow accumulation and melt (e.g., Leung et al., 2003a, b), the Western United States presents an interesting region to study the effects of 3-D radiation on the surface energy and water balance. The surface hydrology of the region has been shown to be sensitive to climate change (Leung et al., 2004; Kapnick and Hall, 2010) and aerosol deposition in snowpack (Qian et al., 2009). Thus, understanding factors leading to uncertainties in modeling snowpack and runoff is important for improving hydrologic predictions from seasonal to century time scales. We present pertinent simulation results in terms of deviations (3-D-PP) of surface solar fluxes and their impact on a number of surface parameters from 1 November 2007 to 31 May 2008 during which abundant snowfall occurred. We focus our analysis on the complex terrains ranging from 1.5 km to above 3 km, which are grouped into four elevation zones.

The organization of the present study is as follows. In Sect. 2, we describe the WRF model used in this investigation, followed by a discussion in Sect. 3 on comparison of 3-D simulation results with available observations for SWE and precipitation. In Sect. 4, we discuss the significance of 3-D radiation effect on the diurnal, monthly, and elevation variation in solar flux, sensible and latent heat fluxes, and surface skin temperature. We do likewise for the monthly averaged surface fluxes, cloud water path, SWE, precipitation, and runoff. Concluding remarks are given in Sect. 5.

2 3-D radiation parameterization in a WRF model

To study the longer term effect of 3-D radiation over mountains/snow, we have employed the WRF model version 3.4 (Skamarock et al., 2008). The relevant model components include the Noah land-surface model (LSM), which is a 4-layer soil temperature and moisture model with canopy moisture and snow cover prediction (Chen and Dudhia, 2001), MM5 surface layer scheme (Paulson, 1970; Dyer and Hicks, 1970; Webb, 1970; Beljaars, 1994; Zhang and Anthes, 1982), Lin scheme for microphysics (Lin et al., 1983), Kain–Fritsch cumulus scheme (Kain and Fritsch, 1990, 1993), and YSU scheme for planetary boundary layer (Hong et al., 2006). For snow-covered surfaces, the Noah LSM considers a mixed snow–vegetation–soil layer and simulates the snow accumulation, sublimation, melting, and heat exchange at the snow–atmosphere and snow–soil interfaces using a simple snow parameterization developed by Koren et al. (1999). The 3-D radiation parameterization follows the approach presented above, which was used in connection with the Fu–Liou–Gu plane-parallel radiation scheme (Fu and Liou, 1992, 1993; Gu et al., 2010, 2011), a scheme which has been included in the WRF physics package.

We have selected a domain covering the Rocky and Sierra Mountains in the Western United States, which is centered at 35° N–120° W and covers the area from 135–102.5° W and 20–45° N. The horizontal grid resolution is 30 km together with a vertical resolution of 28 model levels, the same as discussed in Sect. 1. Initial and boundary conditions are provided by the National Centers for Environmental Prediction (NCEP) Final (FNL) Operational Global Analysis available from the Global Forecast System (GFS) every 6 h on 1.0° × 1.0° grids. Model integrations have been performed starting from 1 November 2007 at 00:00 UTC for a period of 7 months, ending on 31 May 2008, which was selected because the observed snowpack was above the climatological average during this time so that we can assess the effect of 3-D radiative transfer on surface hydrology during a wet year. To investigate the impact of 3-D mountains on surface insolation and snow budget over the Rocky–Sierra regions, we have designed

A WRF simulation of the impact of 3-D radiative transfer

K. N. Liou et al.

Title Page

Abstract

Introduction

Conclusions

References

Tables

Figures



Back

Close

Full Screen / Esc

Printer-friendly Version

Interactive Discussion



**A WRF simulation of
the impact of 3-D
radiative transfer**

K. N. Liou et al.

Title Page

Abstract

Introduction

Conclusions

References

Tables

Figures

◀

▶

◀

▶

Back

Close

Full Screen / Esc

Printer-friendly Version

Interactive Discussion



SWE for the study domain for two elevation zones of 2.5–3 km and > 3 km (Fig. 2c) with the results presented in Rasmussen et al. (2011) (Fig. 2d) for the same cold season starting November 2007. The black dots in Fig. 2d denote the SWE measurements collected at SNOTEL stations typically between 2.4 and 3.6 km in Colorado, and the various curves correspond to WRF simulations performed at a 4 km resolution with various adjustments and averaged over all the SNOTEL locations. Our results at the two elevation zones simulated by the WRF at a 30 km resolution with 3-D radiation parameterization are smaller than the observed SNOTEL data and the 4 km resolution WRF simulations. Considering no specific changes have been made to the WRF model for our simulations as well as the coarser spatial resolution, our results are in reasonable agreement with the control simulation displayed in Fig. 2d.

Moreover, we compared the domain-averaged monthly cumulative precipitation from the 3-D simulation for two elevation zones of 2.5–3 km and > 3 km with the Parameter-elevation Regressions on Independent Slopes Model (PRISM) data (Daly et al., 1994; Taylor et al., 1997), which are averaged results determined from cumulative precipitation measured by 112 SNOTEL sites (Fig. 3a). These sites provide a long-term record of precipitation at high elevations from gauges across the Western United States. The cumulative precipitation increases from November to May, with more precipitation accumulated between December and February. The 30 km resolution model results are larger than, but consistent with, the PRISM values. The daily (0–240 days) precipitation time series from the 3-D simulation is displayed in Fig. 3b, along with the PRISM data. Again, the results reveal that the model reproduced the observed daily variability quite well, but is consistently larger than the PRISM data. Note that our simulations employed the Lin microphysics parameterization, whereas Rasmussen et al. (2011) used the Thompson microphysics parameterization. Thus, differences between the two could be related to microphysics parameterizations, in addition to model resolutions. Overall, however, our simulations capture key features of the daily and seasonal variability as well as the spatial pattern of precipitation and snowpack, which provide confidence for analysis of the impacts of 3-D radiation effects on surface hydrology.

4 Discussions of the 3-D radiation impacts on simulation results

4.1 Diurnal/monthly/elevation variation

The diurnal variation of downward surface solar flux over mountain areas is critically important to regional weather and climate predictions. Figure 4 illustrates simulated deviations in the monthly-averaged downward solar flux at the surface (3-D-PP) for 8 a.m., 12 noon, and 5 p.m. LT in April 2008. The spatial and temporal variations of surface solar flux over the Rocky-Sierra regions are determined by the position of the sun. The averaged solar zenith angles for the month of April corresponding to the three local times are also depicted in the figure. In the early morning, the sun is from the east, and positive deviations are shown on the southeast side of the mountains, while negative values are located in the northwest region. At noon, positive deviations are mostly located south of 38° N and on mountain tops, while negative values are seen north of the mountains, especially in valley areas. In the late afternoon, opposite to the morning hour, increases in solar flux are located on the southwest of the mountains, while decreases in solar fluxes are found in the northeast region.

Deviations (3-D-PP) in the monthly mean domain-averaged diurnal variation time series of downward surface solar flux for a number of elevation ranges, including 1.5–2 km (red), 2–2.5 km (orange), 2.5–3 m (green), above 3 km (blue), as well as the whole domain (black), over the Rocky-Sierra area are shown in Fig. 5 for 6 months (December 2007 to May 2008). Flat lines denote nighttime during which solar insolation is zero. During the winter months (December 2007–February 2008), positive deviations in the surface solar flux are found in the morning (7–10 a.m.) and afternoon (2–5 p.m.), while negative deviations are shown between 10 a.m.–2 p.m. for lower elevations below 2.5 km. For the higher elevation of 2.5–3 km, the negative regions only occur in February. The maximum negative deviation occurs in the lower elevation (1.5–2 km) around noon in February, with a value on the order of 30 W m^{-2} produced by the 3-D mountain effect. During the spring (March–May 2008), positive deviations shifts to earlier morning (6–8 a.m.) while negative deviations begin to occur at 8 a.m. Negative

A WRF simulation of the impact of 3-D radiative transfer

K. N. Liou et al.

Title Page

Abstract

Introduction

Conclusions

References

Tables

Figures



Back

Close

Full Screen / Esc

Printer-friendly Version

Interactive Discussion



**A WRF simulation of
the impact of 3-D
radiative transfer**

K. N. Liou et al.

Title Page

Abstract

Introduction

Conclusions

References

Tables

Figures

◀

▶

◀

▶

Back

Close

Full Screen / Esc

Printer-friendly Version

Interactive Discussion



deviations (3-D–PP) are displayed in Fig. 9c. Because of the cancellation of opposite deviations on the two sides of mountains during morning and afternoon hours, solar flux is enhanced broadly on the south facing side of the mountains south of 38° N and reduced on the north facing side northward of 38° N. In addition, larger increases in solar flux due to 3-D effect are mainly found over mountain tops. Larger reductions, on the other hand, are mostly observed over valley areas between 40–44° N and west of 110° W, where mountains are located in the south and the east. Changes in the surface downward solar flux distribution can affect the formation of clouds, which in turn will impact the transfer of solar flux reaching the surface. Thus, we also examine cloud water path (CWP) produced from experiments 3-D and PP for April 2008. Figure 9b shows the CWP distributions, while Fig. 9d displays deviations (3-D–PP). In reference to Fig. 9d, CWP increases over the mountain summits in the vicinity of northern Rockies where downward solar radiation increases (Fig. 9c), which can enhance the upslope flow and convection, leading to more cloud formation. The increased CWP will in turn partially offset the increased solar radiation over mountain tops.

In Fig. 10a–d, we show deviations (3-D–PP) of the domain-averaged monthly net solar flux, which is defined as the downward solar flux multiplied by $(1 - \bar{A})$, where \bar{A} is the monthly surface albedo, sensible and latent heat fluxes, and surface skin temperature for a 7 month period as a function of elevation. For net solar, sensible heat, and latent heat fluxes over lower elevations (< 2.5 km), negative deviations are shown, with the largest reduction occurring in March. Surface skin temperature largely follows the preceding flux patterns. For higher elevations (> 2.5 km), positive deviations are seen with a minimum between the months of February and March and substantial increases in deviations starting in March associated with the position of the sun. The monthly changes of the whole domain basically follow the pattern of lower elevation ranges (< 2.5 km) which comprises $\sim 65\%$ of the area mentioned previously.

The monthly averaged CWP (gm^{-2}) over the entire domain simulated from the 3-D experiment as a function of elevation is illustrated in Fig. 11a. The corresponding deviations (3-D–PP) are displayed in Fig. 11b. The cloud water over the Rocky–Sierra

A WRF simulation of the impact of 3-D radiative transfer

K. N. Liou et al.

Title Page

Abstract

Introduction

Conclusions

References

Tables

Figures

◀

▶

◀

▶

Back

Close

Full Screen / Esc

Printer-friendly Version

Interactive Discussion



regions appears to generally increase from November and, after reaching a maximum in January, decreases until April and then shows a trend of increasing in May. From November to January, due to the 3-D mountain effect, CWP presents positive changes for the lowest elevation (1.5–2 km) and elevations > 3 km. From January to April, negative deviations occur in all elevation areas. The monthly averaged cloud fraction (%) is shown in Fig. 11c, with the associated deviations depicted in Fig. 11d. Their patterns generally follow those of CWP.

The monthly mean SWE (mm) averaged over the entire domain as a function of elevation is shown in Fig. 12a. The corresponding SWE deviations (3-D–PP) are displayed in Fig. 12d, which show an increase in lower elevations due to the mountain shading effect, with the largest value occurring in March. The positive deviations become smaller after March because the sun is more often overhead during the spring, leading to a reduced shading effect. As a result of increased snow accumulation that reduces rainfall and/or snowmelt contributions to runoff, the cumulative runoff deviations (3-D–PP) are reduced for lower elevation areas (Fig. 12f) with reference to the values produced from the 3-D mountain experiment displayed in Fig. 12c. Due to the mountain effect, SWE decreases over higher elevation areas in connection with greater solar radiation available at the surface. At the elevation range above 3 km, SWE is reduced by 8 % in April and 24 % in May due to 3-D effects. The cumulative runoff increases in February and a maximum increase occurs in April for the elevation range 2.5–3 km, while for elevations above 3 km, the cumulative runoff values substantially increase after March associated with the increased surface solar flux produced by the 3-D mountain effect, leading to increased snowmelt runoff. The surface runoff is calculated from the simple water balance (SWB) model (Schaake et al., 1996). The snow model in the Noah land-surface model simulates the snow accumulation, sublimation, melting, and heat exchange at snow-atmosphere and snow–soil interfaces. The precipitation is grouped as snow when the temperature in the lowest atmospheric layer is below 0 °C.

The monthly mean precipitation (mm) as a function of elevation over the simulation domain is shown in Fig. 12b. Generally precipitation increases with elevation due to

A WRF simulation of the impact of 3-D radiative transfer

K. N. Liou et al.

Title Page

Abstract

Introduction

Conclusions

References

Tables

Figures

◀

▶

◀

▶

Back

Close

Full Screen / Esc

Printer-friendly Version

Interactive Discussion



orographic forcing except above 3 km where moisture is significantly depleted due to rainout at the lower elevations. Precipitation increases from November to May with substantially larger values for elevation areas higher than 2.5 km. In terms of deviations (3-D-PP), we see decreases in higher elevation areas, with a minimum occurring in April in relation to the CWP deviation result (Fig. 11b), which also contributes to SWE decrease. For lower regions, precipitation deviations (Fig. 12e) increase and result in the increased SWE in conjunction with the reduced runoff. Thus, one important impact of the 3-D mountain effect is to delay the snowmelt-driven runoff into the warm season for lower elevations and, at the same time, to enhance the SWE in higher elevation regions.

5 Concluding remarks

The 3-D radiative transfer parameterization developed for the computation of surface solar fluxes has been incorporated into the WRF model and applied at a resolution of 30 km over the Rocky–Sierra Mountains in the Western United States. We have carried out simulations for a seven-month period from 1 November 2007 to 31 May 2008, during which snow accumulation was abundant, to understand the effect of 3-D mountains/snow on the diurnal and monthly variation of surface radiative and heat fluxes and the consequence of snowmelt and precipitation on different elevations. The monthly mean SWE values from the WRF simulation with 3-D radiation are generally comparable in spatial pattern and seasonality to the CMC and SNOTEL data. In view of the relatively coarse resolution of 30 km compared to the WRF simulations performed at a 4 km resolution presented by Rasmussen et al. (2011), our simulated SWE is high in magnitude. This is confirmed by comparing our simulated precipitation at high elevation zones (higher than 2.5 km) with SNOTEL data, which are also obtained at high elevations. Nevertheless, our simulations captured the spatial pattern, elevation dependence, and daily/seasonal variability of precipitation and snowpack sufficiently well to provide confidence for investigating the impacts of 3-D radiation associated with moun-

tains/snow on the surface hydrology of the Western United States. Key findings are summarized as follows.

First, deviations of the monthly mean surface solar flux produced by 3-D mountain effects compared to PP results over the Rocky–Sierra Mountain regions are a function of elevation and time of the day. During winter, positive deviations up to 10 W m^{-2} are found in the morning from 7–10 a.m. as well as in the afternoon from 2–5 p.m. due to shading effects for areas at elevations below 2.5 km. The maximum negative deviation occurs in the lower elevation from 1.5–2 km around noon in February with a value of $\sim 30 \text{ W m}^{-2}$. During spring, positive deviations shifts to earlier morning (between 6–8 a.m.), while negative deviations begin to occur at 8 a.m. Over the mountain tops above 3 km, positive deviations are found throughout the day, indicating that more solar fluxes are available in this region in association with longer daylight hours. The maximum positive deviation is found around noon in May, with a value of $\sim 60 \text{ W m}^{-2}$.

Second, deviations in the surface solar radiation field can affect latent and sensible heat fluxes, and the changes in the surface energy balance are reflected in changes in surface skin temperature. Changes in the seasonal sensible and latent heat fluxes as functions of local time and elevation primarily follow net solar flux patterns. Also, negative (winter) and positive (spring) deviations in sensible/latent heat fluxes become smaller in magnitude around noon. The deviations in sensible heat flux are generally greater than that of latent heat flux, which reflect the bowen ratio in the semi-arid Western United States. We obtained a maximum of $\sim 30 \text{ W m}^{-2}$ around noon for sensible heat flux compared to $\sim 10 \text{ W m}^{-2}$ for latent heat flux in May. Deviations in the surface skin temperature, which largely follows the diurnal net solar flux pattern, displays cooling for elevations below 2.5 km due to shading effects. For mountain top regions ($> 3 \text{ km}$), warming is found throughout the day for both winter and spring.

Third, the monthly SWE deviations averaged over the entire domain show an increase in lower elevations due to the mountain shading effect, which produces the largest value in March (a 15 % increase at the lowest elevation range of 1.5–2 km) and positive deviations become smaller during other spring months associated with the

A WRF simulation of the impact of 3-D radiative transfer

K. N. Liou et al.

Title Page

Abstract

Introduction

Conclusions

References

Tables

Figures



Back

Close

Full Screen / Esc

Printer-friendly Version

Interactive Discussion



A WRF simulation of the impact of 3-D radiative transfer

K. N. Liou et al.

Title Page

Abstract

Introduction

Conclusions

References

Tables

Figures

◀

▶

◀

▶

Back

Close

Full Screen / Esc

Printer-friendly Version

Interactive Discussion



position of overhead sun. The cumulative runoff is subsequently reduced in lower elevation areas from February to May due to the mountain effect that reduces snowmelt. On the contrary, over higher elevation areas, SWE decreases by 8–24 % in April and May in connection with more solar radiation available at the surface. As a result of increased snowmelt, the cumulative runoff increases in spring with a maximum increase occurring in April for the elevation range 2.5–3 km. At the mountain tops above 3 km, the cumulative runoff values substantially increase after March associated with the increased surface solar flux produced by the 3-D mountain effect, leading to increased snowmelt runoff. Precipitation decreases from November to May with substantially larger deviations at elevation higher than 2.5 km. For lower elevation regions, precipitation increases and contributes to the increased SWE due to shading effects. Thus, an important impact of the 3-D mountain effect is to enhance (reduce) the SWE in lower (higher) elevation regions, while concurrently shifting the runoff seasonality through changes in snowmelt.

Overall, this study shows that deviations of SWE due to 3-D radiation effects range from an increase of 18 % at the lowest elevation range (1.5–2 km) to a decrease of 8 % at the highest elevation range (> 3 km) during the snowmelt season of April to May. Because lower elevation areas occupy larger fractions of the land surface, the net effect of 3-D radiation is to extend snowmelt and snowmelt-driven runoff into the warm season. The redistribution of SWE across elevation and shift in runoff timing have important implications to cold season surface hydrology that may extend through the warm season due to changes in soil moisture and evapotranspiration. Since about 60–90 % of water resources originate from mountains worldwide, the aforementioned differences in simulated hydrology due solely to 3-D interactions between solar radiation and mountains merit further investigation in order to understand the implications to modeling mountain water resources and their vulnerability to climate change and air pollution.

We have focused in this study on analysis involving the interactions between solar radiation and surface energy and water budgets by means of elevation bands. As a follow-up study, we plan to investigate the 3-D mountain orientation effect on the dis-

A WRF simulation of the impact of 3-D radiative transfer

K. N. Liou et al.

Title Page

Abstract

Introduction

Conclusions

References

Tables

Figures

◀

▶

◀

▶

Back

Close

Full Screen / Esc

Printer-friendly Version

Interactive Discussion



tributions of surface solar and heat fluxes, SWE, runoff, and precipitation on the basis of simulations presented above. It would also be interesting to study surface hydrological patterns in relation to the 3-D mountain radiation effect in the summer months to investigate how changes in surface energy and hydrology associated with SWE, runoff, and soil moisture influence evapotranspiration patterns in the summer, as well as how diurnal deviations of solar radiation due to mountains influence convection and the diurnal timing and amount of precipitation.

Acknowledgements. This research was supported by the Office of Science of the US Department of Energy as part of the Earth System Modeling program through DOE Grant DESC0006742 to UCLA and separate funding to PNNL. PNNL is operated for DOE by Battelle Memorial Institute under contract DE-AC05-76RLO1830.

References

- Beljaars, A. C. M.: The parameterization of surface fluxes in large-scale models under free convection, *Q. J. Roy. Meteor. Soc.*, 121, 255–270, 1994.
- Bonan, G. B.: *Ecological Climatology: Concepts and Applications*, Cambridge Univ. Press, New York, USA, 678 pp., 2002.
- Brown, R. D. and Brasnett, B.: Canadian Meteorological Centre (CMC) Daily Snow Depth Analysis Data, Environment Canada, 2010, Boulder, CO, USA: National Snow and Ice Data Center (updated annually), 2010.
- Chen, F. and Dudhia, J.: Coupling an advanced land surface-hydrology model with the Penn State-NCAR MM5 modeling system. Part I: Model implementation and sensitivity, *Mon. Weather Rev.*, 129, 569–585, 2001.
- Chen, Y., Hall, A., and Liou, K. N.: Application of three-dimensional solar radiative transfer to mountains, *J. Geophys. Res.*, 111, D21111, doi:10.1029/2006JD007163, 2006.
- Daly, C., Neilson, R. P., and Phillips, D. L.: A statistical-topographical model for mapping climatological precipitation over mountainous terrain, *J. Appl. Meteorol.*, 33, 140–158, 1994.
- Dyer, A. J. and Hicks, B. B.: Flux–gradient relationships in the constant flux layer, *Q. J. Roy. Meteor. Soc.*, 96, 715–721, 1970.

A WRF simulation of the impact of 3-D radiative transfer

K. N. Liou et al.

Title Page

Abstract

Introduction

Conclusions

References

Tables

Figures

◀

▶

◀

▶

Back

Close

Full Screen / Esc

Printer-friendly Version

Interactive Discussion



- Fu, Q. and Liou, K. N.: On the correlated k -distribution method for radiative transfer in nonhomogeneous atmospheres, *J. Atmos. Sci.*, 49, 2139–2156, 1992.
- Fu, Q. and Liou, K. N.: Parameterization of the radiative properties of cirrus clouds, *J. Atmos. Sci.*, 50, 2008–2025, 1993.
- 5 Geiger, R.: *The Climate Near the Ground*, Harvard Univ. Press, Cambridge, USA, 611 pp., 1965.
- Gu, L., Baldocchi, D., Verma, S. B., Black, T. A., Vesala, T., Falge, E. M., and Dowty, P. R.: Advantages of diffuse radiation for terrestrial eco-system productivity, *J. Geophys. Res.*, 107, 4050, doi:10.1029/2001JD001242, 2002.
- 10 Gu, Y., Liou, K. N., Chen, W., and Liao, H.: Direct climate effect of black carbon in China and its impact on dust storms, *J. Geophys. Res.*, 115, D00K14, 2010.
- Gu, Y., Liou, K. N., Ou, S. C., and Fovell, R.: Cirrus cloud simulations using WRF with improved radiation parameterization and increased vertical resolution, *J. Geophys. Res.*, 116, D06119, doi:10.1029/2010JD014574, 2011.
- 15 Gu, Y., Liou, K. N., Lee, W.-L., and Leung, L. R.: Simulating 3-D radiative transfer effects over the Sierra Nevada Mountains using WRF, *Atmos. Chem. Phys.*, 12, 9965–9976, doi:10.5194/acp-12-9965-2012, 2012.
- Hong, S.-Y., Noh, Y., and Dudhia, J.: A new vertical diffusion package with an explicit treatment of entrainment processes, *Mon. Weather Rev.*, 134, 2318–2341, 2006.
- 20 Kain, J. S. and Fritsch, J. M.: A one-dimensional entraining/detraining plume model and its application in convective parameterization, *J. Atmos. Sci.*, 47, 2784–2802, 1990.
- Kain, J. S. and Fritsch, J. M.: Convective parameterization for mesoscale models: the Kain–Fritsch scheme, in: *The Representation of Cumulus Convection in Numerical Models*, edited by: Emanuel, K. A. and Raymond, D. J., Amer. Meteor. Soc., 246 pp., 1993.
- 25 Kapnick, S. and Hall, A.: Observed climate–snowpack relationships in California and their implications for the Future, *J. Climate*, 23, 3446–3456, 2010.
- Koren, V., Schaake, J., Mitchell, K., Duran, Q. Y., Chen, F., and Baker, J. M.: A parameterization of snowpack and frozen ground intended for NCEP weather and climate models, *J. Geophys. Res.*, 104, 19569–19585, 1999.
- 30 Lee, W. L., Liou, K. N., and Hall, A.: Parameterization of solar fluxes over mountain surfaces for application to climate models, *J. Geophys. Res.*, 116, D01101, doi:10.1029/2010JD014722, 2011.

A WRF simulation of the impact of 3-D radiative transfer

K. N. Liou et al.

Title Page

Abstract

Introduction

Conclusions

References

Tables

Figures

◀

▶

◀

▶

Back

Close

Full Screen / Esc

Printer-friendly Version

Interactive Discussion



Lee, W. L., Liou, K. N., and Wang, C.: Impact of 3-D topography on surface radiation budget over the Tibetan Plateau, *Theor. Appl. Climatol.*, 113, 95–103, doi:10.1007/s00704-012-0767-y, 2012.

Leung, L. R., Qian, Y., and Bian, X.: Hydroclimate of the western United States based on observations and regional climate simulation of 1981–2000. Part I: Seasonal statistics, *J. Climate*, 16, 1892–1991, 2003a.

Leung, L. R., Qian, Y., Bian, X., and Hunt, A.: Hydroclimate of the western United States based on observations and regional climate simulation of 1981–2000. Part II: Mesoscale ENSO anomalies, *J. Climate*, 16, 1912–1928, 2003b.

Leung, L. R., Qian, Y., Bian, X., Washington, W. M., Han, J., and Roads, J. O.: Mid-century ensemble regional climate change scenarios for the western United States, *Clim. Change*, 62, 75–113, 2004.

Lin, Y.-L., Farley, R. D., and Orville, H. D.: Bulk parameterization of the snow field in a cloud model, *J. Clim. Appl. Meteorol.*, 22, 1065–1092, 1983.

Liou, K. N., Lee, W.-L., and Hall, A.: Radiative transfer in mountains: application to the Tibetan Plateau, *Geophys. Res. Lett.*, 34, L23809, doi:10.1029/2007GL031762, 2007.

Müller, M. D. and Scherer, D.: A grid- and subgrid-scale radiation parameterization of topographic effects for mesoscale weather forecast models, *Mon. Weather Rev.*, 133, 1431–1442, 2005.

Paulson, C. A.: The mathematical representation of wind speed and temperature profiles in the unstable atmospheric surface layer, *J. Appl. Meteorol.*, 9, 857–861, 1970.

Qian, Y., Gustafson, W. I., Leung, L. R., and Ghan, S. J.: Effects of soot-induced snow albedo change on snowpack and hydrological cycle in western US based on WRF chemistry and regional climate simulations, *J. Geophys. Res.*, 114, D03108, doi:10.1029/2008JD011039, 2009.

Rasmussen, R. M., Liu, C., Ikeda, K., Gochis, D., Yates, D., Chen, F., Tewari, M., Barlage, M., Dudhia, J., Yu, W., Miller, K., Arsenault, K., Grubistic, V., Thompson, G., and Gutmann, E.: Weather Support to Deicing Decision Making (WSDDM): a winter weather nowcasting system, *B. Am. Meteorol. Soc.*, 82, 579–595, 2011.

Schaake, J. C., Koren, V. I., Duan, Q. Y., Mitchell, K., and Chen, F.: A simple water balance model (SWB) for estimating runoff at different spatial and temporal scales, *J. Geophys. Res.*, 101, 7461–7475, 1996.

A WRF simulation of the impact of 3-D radiative transfer

K. N. Liou et al.

Title Page

Abstract

Introduction

Conclusions

References

Tables

Figures

◀

▶

◀

▶

Back

Close

Full Screen / Esc

Printer-friendly Version

Interactive Discussion



Skamarock, W. C., Klemp, J. B., Dudhia, J., Gill, D. O., Barker, D. M., Wang, W., and Powers, J. G.: A description of the Advanced Research WRF Version 2, NCAR Tech. Note 468+STR, Natl. Cent. for Atmos. Res., Boulder, CO, USA, 88 pp., 2005.

5 Skamarock, W. C., Klemp, J. B., Dudhia, J., Gill, D. O., Barker, D. M., Wang, W., and Powers, J. G.: A description of the Advanced Research WRF Version 3, NCAR Tech. Note 475+STR, 125 pp., Natl. Cent. for Atmos. Res., Boulder, CO, USA, 2008.

Taylor, G., Daly, C., Gibson, W., and Sibul-Weisburg, J.: Digital and Map Products Produced Using PRISM, in: 10th Conf. on Applied Climatology, Reno, NV, Amer. Meteor. Soc., 217–218, 1997.

10 Webb, E. K.: Profile relationships: the log-linear range and extension to strong stability, Q. J. Roy. Meteor. Soc., 96, 67–90, 1970.

Zhang, D.-L. and Anthes, R. A.: A high-resolution model of the planetary boundary layer-sensitivity tests and comparisons with SESAME-79 data, J. Appl. Meteorol., 21, 1594–1609, 1982.

A WRF simulation of the impact of 3-D radiative transfer

K. N. Liou et al.

Title Page

Abstract

Introduction

Conclusions

References

Tables

Figures



Back

Close

Full Screen / Esc

Printer-friendly Version

Interactive Discussion



Terrain Height (m): 30 x 30 km² Resolution

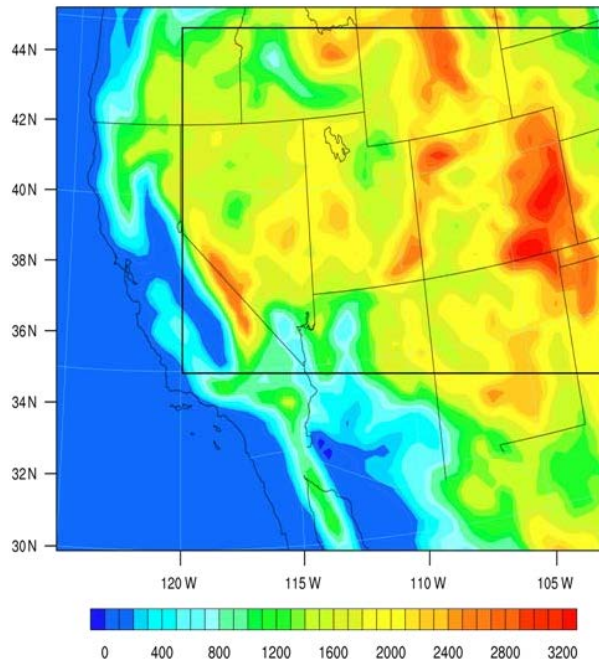


Fig. 1. The elevation map over a 30 km resolution grid for the Rocky–Sierra areas in the Western United States. The box on the map displays major mountainous areas where simulation results are analyzed and presented in the paper.

A WRF simulation of the impact of 3-D radiative transfer

K. N. Liou et al.

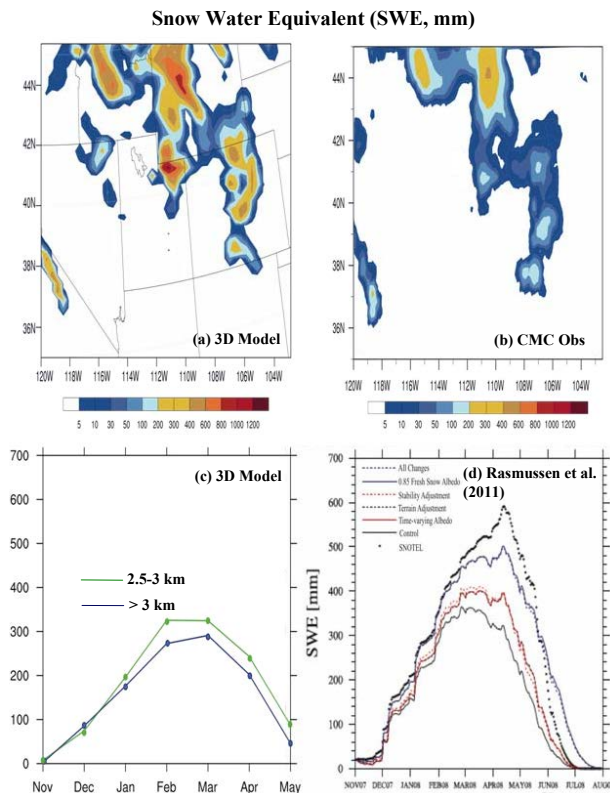


Fig. 2. (a) The monthly mean SWE map (5–1200 mm, see Fig. 1) for April 2008 simulated from the WRF with the inclusion of 3-D radiation parameterization. (b) The monthly mean SWE values estimated from the Northern Hemisphere daily snow depth analysis data processed by the Canadian Meteorological Centre (CMC). (c) The monthly time series of SWE for the study domain for two elevation zones of 2.5–3 km and > 3 km. (d) The monthly time series of SWE presented in Rasmussen et al. (2011). The black dots denote the SWE measurements collected at stations typically between 2.4 and 3.6 km in Colorado.

A WRF simulation of the impact of 3-D radiative transfer

K. N. Liou et al.

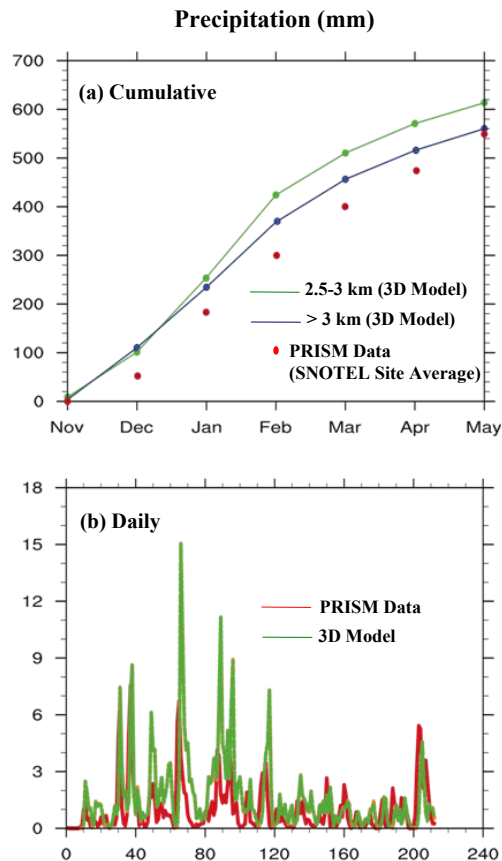


Fig. 3. (a) The domain-averaged monthly cumulative precipitation simulated from the present model for two elevation zones of 2.5–3 km and > 3 km with the Parameter-elevation Regressions on Independent Slopes Model (PRISM) data, which are the averaged results determined from cumulative precipitation measured from 112 SNOTEL sites. (b) The daily (0–240 days) precipitation time series computed from the 3-D model, along with the PRISM data.

Downward Solar Flux Deviations (3D – PP)

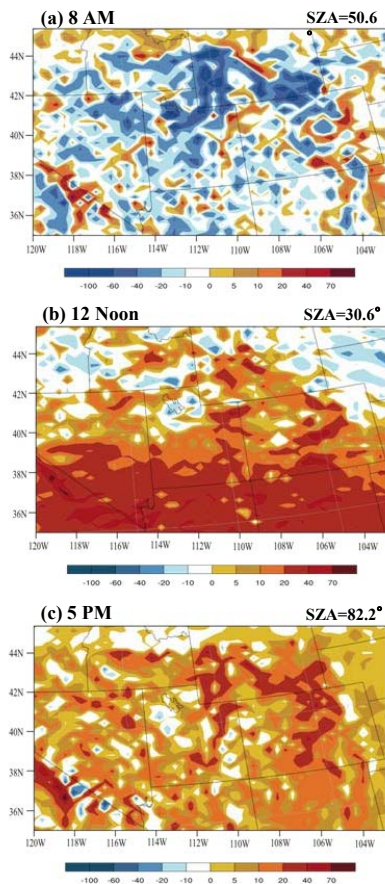


Fig. 4. Deviations (3-D–PP) in the monthly averaged downward surface solar flux distributions in $W m^{-2}$ for 8 a.m., 12 noon, and 5 p.m. LT in April 2008 (see the box in Fig. 1). The solar flux scale ranges from -100 to $+70 W m^{-2}$.

A WRF simulation of the impact of 3-D radiative transfer

K. N. Liou et al.

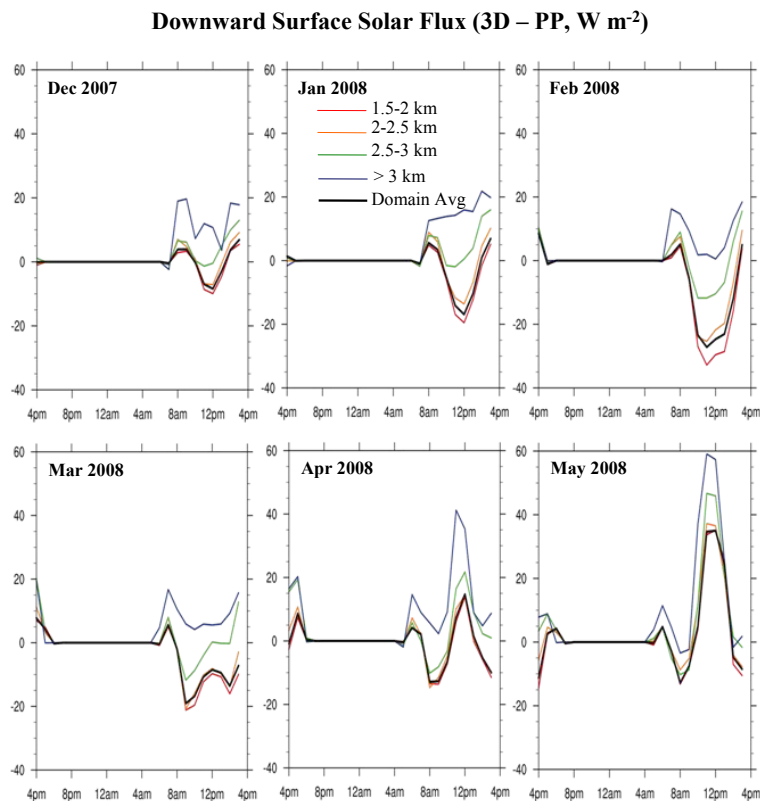


Fig. 5. Deviations (3-D-PP) in the monthly mean domain-averaged diurnal variation time series of surface solar flux for a number of elevation ranges, including 1.5–2 km (red), 2–2.5 km (orange), 2.5–3 m (green), above 3 km (blue), as well as the whole domain (black), over the Rocky–Sierra area for 6 months (December 2007 to May 2008). Flat lines denote nighttime during which solar insolation is zero.

[Title Page](#)
[Abstract](#)
[Introduction](#)
[Conclusions](#)
[References](#)
[Tables](#)
[Figures](#)
[◀](#)
[▶](#)
[◀](#)
[▶](#)
[Back](#)
[Close](#)
[Full Screen / Esc](#)
[Printer-friendly Version](#)
[Interactive Discussion](#)


A WRF simulation of the impact of 3-D radiative transfer

K. N. Liou et al.

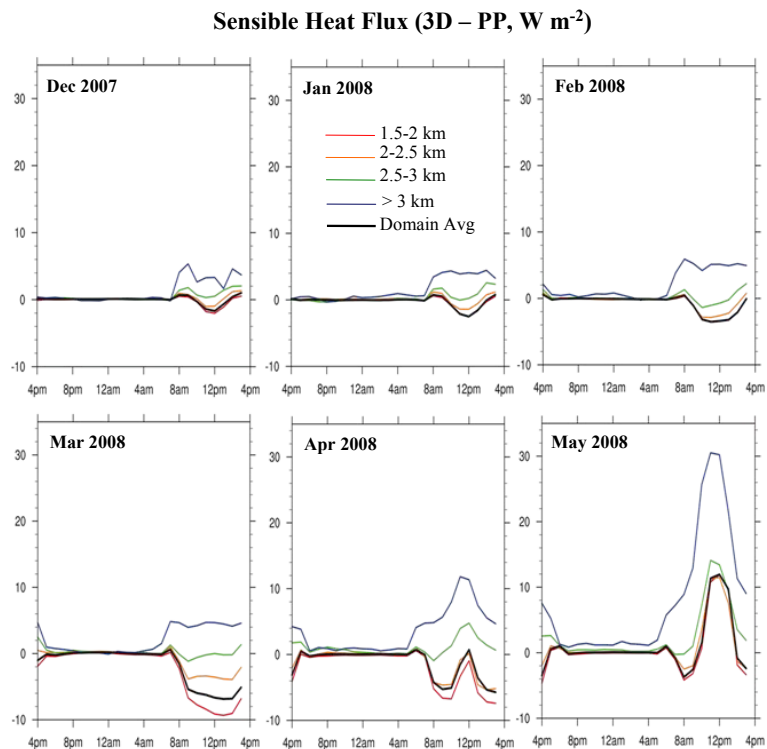


Fig. 6. Same as in Fig. 5, except for the monthly mean domain-averaged diurnal variation time series of sensible heat flux.

[Title Page](#)[Abstract](#)[Introduction](#)[Conclusions](#)[References](#)[Tables](#)[Figures](#)[◀](#)[▶](#)[◀](#)[▶](#)[Back](#)[Close](#)[Full Screen / Esc](#)[Printer-friendly Version](#)[Interactive Discussion](#)

**A WRF simulation of
the impact of 3-D
radiative transfer**

K. N. Liou et al.

Title Page

Abstract

Introduction

Conclusions

References

Tables

Figures

◀

▶

◀

▶

Back

Close

Full Screen / Esc

Printer-friendly Version

Interactive Discussion

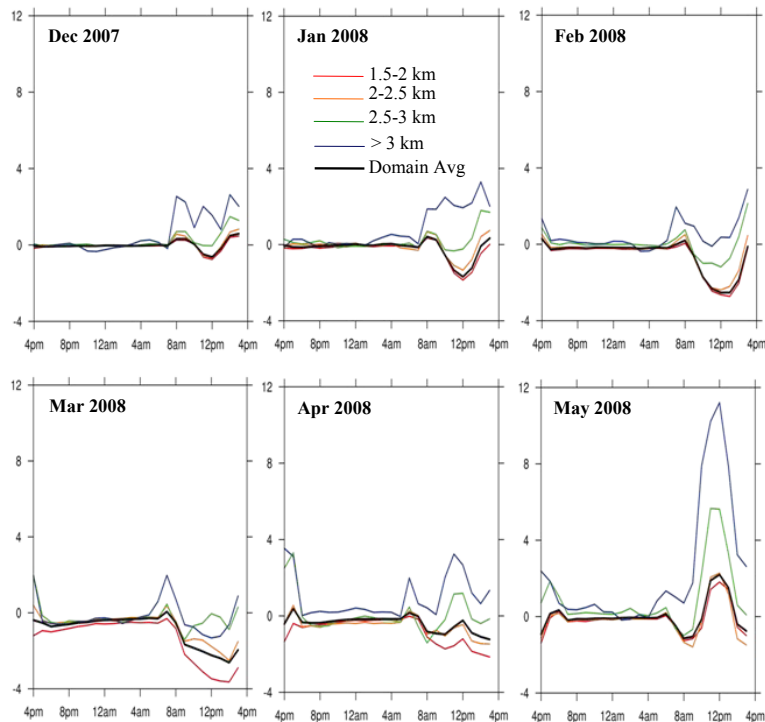
**Latent Heat Flux (3D – PP, W m⁻²)**

Fig. 7. Same as in Fig. 5, except for the monthly mean domain-averaged diurnal variation time series of latent heat flux.

A WRF simulation of the impact of 3-D radiative transfer

K. N. Liou et al.

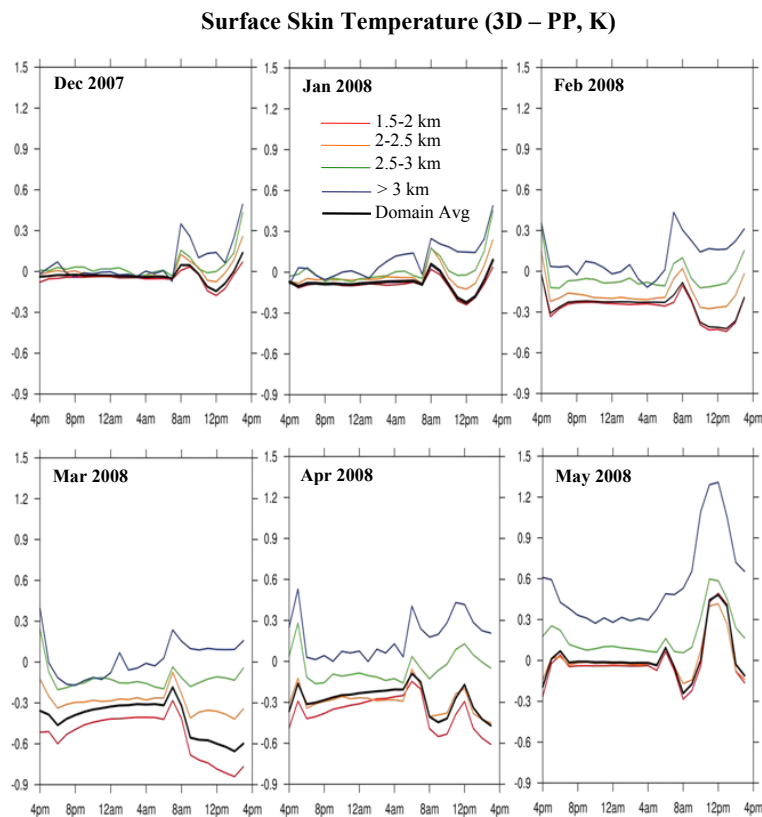


Fig. 8. Same as in Fig. 5, except for the monthly mean domain-averaged diurnal variation time series of surface skin temperature.

[Title Page](#)[Abstract](#)[Introduction](#)[Conclusions](#)[References](#)[Tables](#)[Figures](#)[◀](#)[▶](#)[◀](#)[▶](#)[Back](#)[Close](#)[Full Screen / Esc](#)[Printer-friendly Version](#)[Interactive Discussion](#)

Downward Solar Flux (W m^{-2}) April 2008 Cloud Water Path (g m^{-2})

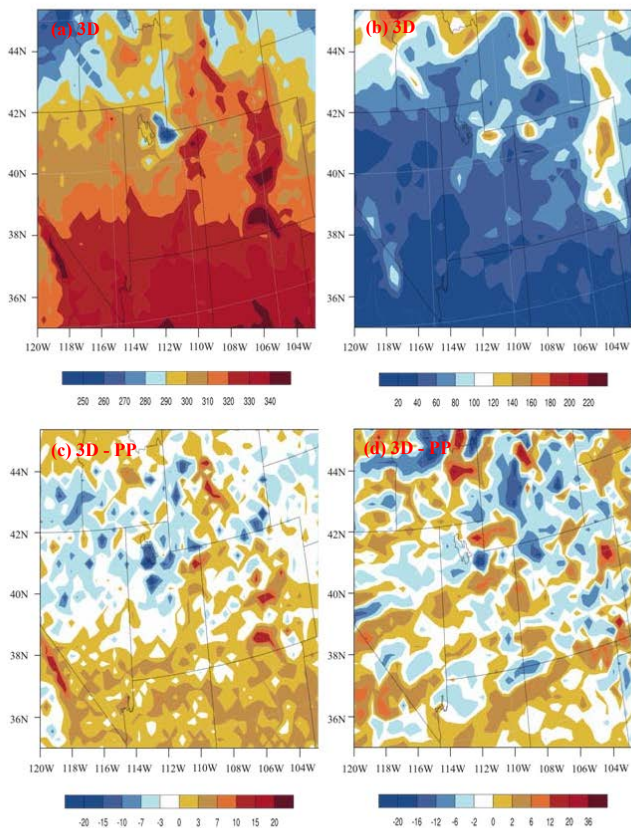


Fig. 9. (a) The monthly averaged surface solar flux (W m^{-2}) map for April 2008 simulated for the 3-D case as a function of latitude and longitude. (b) The monthly averaged Cloud Water Path (CWP, g m^{-2}) map for April 2008 simulated for the 3-D case as a function of latitude and longitude. (c) The corresponding deviation (3-D-PP) map for downward solar flux. (d) The corresponding deviation (3-D-PP) map for CWP.

A WRF simulation of the impact of 3-D radiative transfer

K. N. Liou et al.

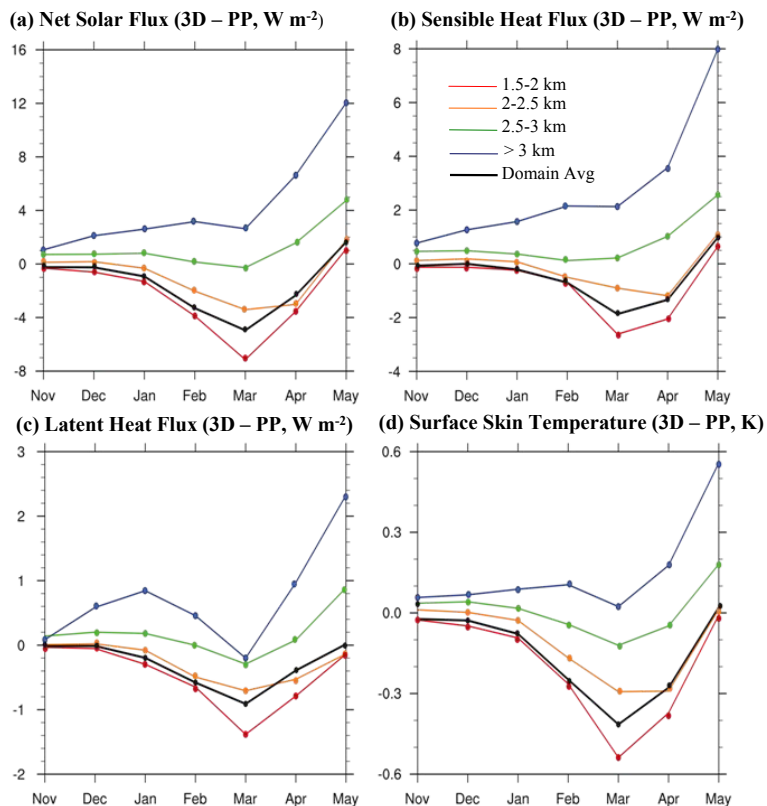


Fig. 10. Deviations (3D–PP) of the domain-averaged monthly (a) net solar flux, (b) sensible heat flux, (c) latent heat flux, and (d) surface skin temperature for a 7 month period (November 2007–May 2008) as a function of elevation. 1.5–2 km (red), 2–2.5 km (orange), 2.5–3 m (green), above 3 km (blue), and the whole domain (black).

Title Page

Abstract Introduction

Conclusions References

Tables Figures

◀ ▶

◀ ▶

Back Close

Full Screen / Esc

Printer-friendly Version

Interactive Discussion



A WRF simulation of the impact of 3-D radiative transfer

K. N. Liou et al.

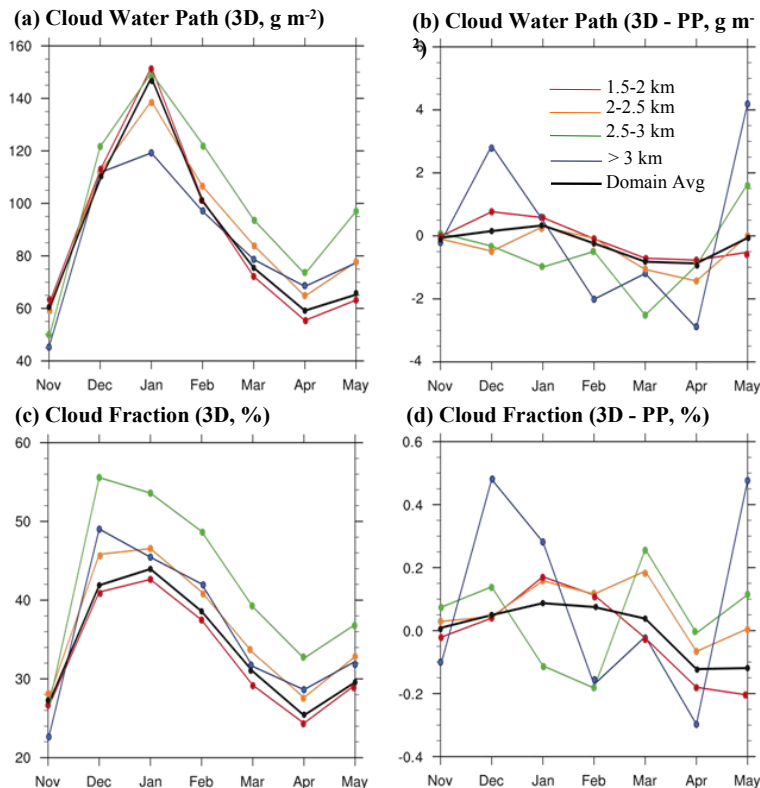


Fig. 11. (a) The monthly averaged Cloud Water Path (CWP, g m^{-2}) over the entire domain simulated from the 3-D experiment as a function of elevation. (b) The corresponding deviations (3-D-PP) for CWP. (c) The monthly averaged cloud fraction (%) over the entire domain simulated from the 3-D experiment as a function of elevation. (d) The corresponding deviations (3-D-PP) for cloud fraction. 1.5–2 km (red), 2–2.5 km (orange), 2.5–3 m (green), above 3 km (blue), and the whole domain (black).

A WRF simulation of the impact of 3-D radiative transfer

K. N. Liou et al.

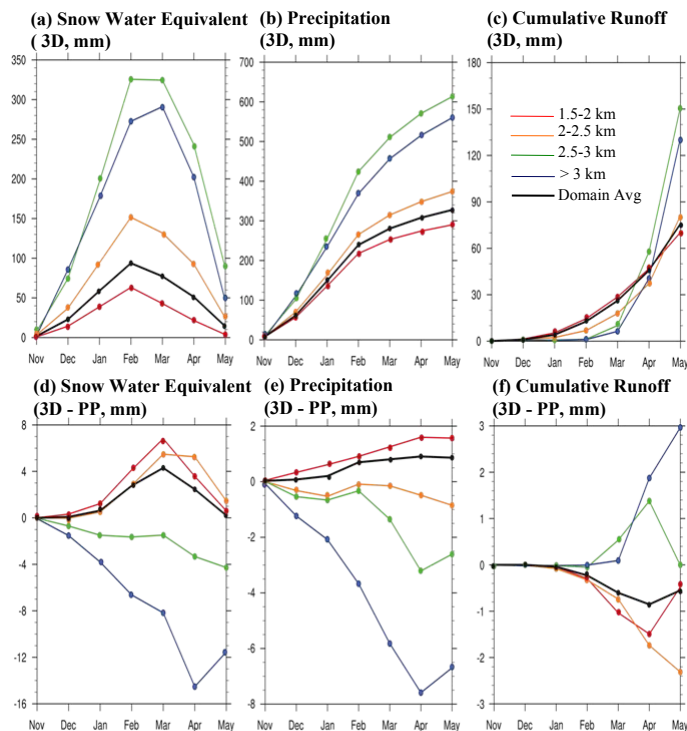


Fig. 12. (a) The monthly mean Snow Water Equivalent (SWE, mm) averaged over the simulation domain as a function of elevation. (b) The monthly mean precipitation (mm) averaged over the simulation domain as a function of elevation. (c) The monthly mean cumulative runoff averaged over the simulation domain as a function of elevation. (d) The corresponding SWE deviations (3-D-PP). (e) The correspondence precipitation deviations (3-D-PP). (f) The correspondence runoff deviations (3-D-PP). 1.5–2 km (red), 2–2.5 km (orange), 2.5–3 m (green), above 3 km (blue), and the whole domain (black).

[Title Page](#)
[Abstract](#)
[Introduction](#)
[Conclusions](#)
[References](#)
[Tables](#)
[Figures](#)
[Back](#)
[Close](#)
[Full Screen / Esc](#)
[Printer-friendly Version](#)
[Interactive Discussion](#)
